



HAL
open science

A second order cell centered scheme for convection-diffusion equations on unstructured non-conforming grids

Libuse Piar, Fabrice Babik, Raphaele Herbin, Jean-Claude Latché

► **To cite this version:**

Libuse Piar, Fabrice Babik, Raphaele Herbin, Jean-Claude Latché. A second order cell centered scheme for convection-diffusion equations on unstructured non-conforming grids. 2011. hal-00556911v1

HAL Id: hal-00556911

<https://hal.science/hal-00556911v1>

Preprint submitted on 23 Jan 2011 (v1), last revised 3 Dec 2012 (v2)

HAL is a multi-disciplinary open access archive for the deposit and dissemination of scientific research documents, whether they are published or not. The documents may come from teaching and research institutions in France or abroad, or from public or private research centers.

L'archive ouverte pluridisciplinaire **HAL**, est destinée au dépôt et à la diffusion de documents scientifiques de niveau recherche, publiés ou non, émanant des établissements d'enseignement et de recherche français ou étrangers, des laboratoires publics ou privés.

A second order cell centered scheme for convection-diffusion equations on unstructured non-conforming grids

L. Piar^a, F. Babik^a, R. Herbin^b, J.-C. Latché^{a*}

^a *Institut de Radioprotection et de Sûreté Nucléaire (IRSN)*
email: [libuse.piar, fabrice.babik, jean-claude.latche]@irsn.fr

^b *Université de Provence – email: herbin@cmi.univ-mrs.fr*

SUMMARY

We propose in this paper a finite volume scheme to compute the solution of convection-diffusion equation on unstructured and non-conforming grids. The diffusive fluxes are approximated using the recently published SUSHI scheme in its cell centred version, that reaches a second order spatial convergence rate for the Laplace equation on any unstructured 2D/3D grids. As in the MUSCL method, the numerical convective fluxes are built with a prediction-limitation process which ensures that the discrete maximum principle is satisfied for pure convection problems. The limitation does not involve any geometrical reconstruction, thus allowing the use of completely general grids, in any space dimension.

KEY WORDS: Finite Volumes, MUSCL method, convection dominant regime, discrete maximum principle, convergence analysis

1. Introduction

In this paper, we address the following convection–diffusion problem:

$$\partial_t \bar{u} + \operatorname{div}(\bar{u}\mathbf{v}) - \operatorname{div}(\kappa \nabla \bar{u}) = f \quad \text{on } \Omega \times (0, T), \quad (1a)$$

$$\bar{u}(\mathbf{x}, t) = \bar{u}_D(\mathbf{x}, t) \quad \text{on } \partial\Omega_D \times (0, T), \quad (1b)$$

$$-\kappa \nabla \bar{u}(\mathbf{x}, t) \cdot \mathbf{n} = g_N(\mathbf{x}, t) \quad \text{on } \partial\Omega_N \times (0, T), \quad (1c)$$

$$\bar{u}(\mathbf{x}, 0) = \bar{u}_0(\mathbf{x}) \quad \text{in } \Omega, \quad (1d)$$

where $\Omega \subset \mathbb{R}^d$, $d = 1, 2, 3$, is an open connected and bounded domain supposed to be polygonal ($d = 2$) or polyhedral ($d = 3$), \mathbf{v} is a divergence-free velocity field, κ is a non-negative constant real number and $f \in L^2(\Omega \times (0, T))$ is a given source term. The boundary $\partial\Omega$ of Ω is split into $\partial\Omega_D$ and $\partial\Omega_N$ (the so-called Dirichlet and Neumann boundaries), which form a partition of $\partial\Omega$, and satisfy (i) that the measure of $\partial\Omega_D$ is positive and (ii) that $\mathbf{v} \cdot \mathbf{n} \geq 0$ on $\partial\Omega_N$, where \mathbf{n} is the unit normal vector to $\partial\Omega$ outward Ω . If $\kappa = 0$, we suppose in addition that $\mathbf{v} \cdot \mathbf{n} \leq 0$ on $\partial\Omega_D$, that is, as usual for the transport equation, that $\partial\Omega_D$ is the inflow part of the boundary and $\partial\Omega_N$ the outflow one. The functions \bar{u}_0 , \bar{u}_D and g_N denote the initial value, the Dirichlet boundary value and the diffusion flux prescribed at the Neumann boundary, respectively.

January 2011

In this paper, we propose a cell-centred scheme for the solution of (1), able to cope with almost arbitrary meshes.

The diffusion term is discretized by a cell centred scheme which was first presented in [10] and tested in [1] for oil engineering simulation problems. Its convergence analysis was performed in [9] in the framework of its more general version SUSHI (Scheme Using Stabilization and Hybrid Interfaces) for the discretization of anisotropic and heterogeneous diffusion problems on general non-conforming grids. This scheme is implemented here with a minor variant for the approximation of Neumann boundary conditions, which completely eliminates the unknowns at the faces of the mesh (including boundary faces), thus restricting the set of the unknowns to the cell values only.

For the convection term, we use a finite volume approach, based, as in MUSCL-type schemes, on a two-step algorithm: we first compute a tentative approximation of the unknown field at the face by an affine reconstruction, then modify it (by a so-called limitation procedure) to ensure the L^∞ -stability of the scheme. The development of this type of schemes has been the subject of a huge amount of literature; we refer to [18, 12, 16] for seminal works for one-dimensional problems, [3] for a review of the adaptation of these ideas in multi-dimensional spaces, and [14, 5, 4] for recent works. In these approaches, the limitation procedure is presented as a limitation of the slope defined by the cell and face values, on the basis of its comparison with other slopes defined by the values taken by the unknown in the neighbourhood. Then, under geometric assumptions for the mesh, this limitation may be shown to imply some conditions (let us call them *stability conditions*) for the approximation at the face which ensure, for pure convection problems, a local maximum principle [8, 7]. Our strategy here (see also [17] for an ongoing related work) is based on the following remark: for a linear convection term, these *stability conditions* may be exploited to define an admissible interval for the value at the face. This suggests a crude limitation process, which does not use any slope computation and simply consists in performing a (one-dimensional) projection of the tentative affine reconstructed face value on this interval. In addition, *stability conditions* are purely algebraic (in the sense that they do not require any geometric computation), and thus work with arbitrary meshes.

This paper is organized as follows. We first introduce some definitions and notations for the mesh (Section 2). We then describe the scheme (Section 3), the discretization of the diffusion and convection terms being detailed in Section 3.1 and Section 3.2 respectively. We conclude by some numerical tests (Section 4).

2. The mesh

A finite volume discretization of Ω is defined by a triplet $(\mathcal{M}, \mathcal{E}, \mathcal{P})$, where:

- \mathcal{M} is a set of non-empty convex open disjoint subsets K of Ω (the control volumes), such that $\bar{\Omega} = \bigcup_{K \in \mathcal{M}} \bar{K}$.
- \mathcal{E} is the set of edges (in 2D) or faces (in 3D), denoted by σ . We denote by $\mathcal{E}(K) \subset \mathcal{E}$ the set of faces of $K \in \mathcal{M}$, by \mathcal{E}_{ext} and \mathcal{E}_{int} the set of boundary and interior faces, respectively. Each $\sigma \in \mathcal{E}_{\text{int}}$ is supposed to have exactly two neighbouring cells, say $K, L \in \mathcal{M}$, and $\bar{K} \cap \bar{L} = \bar{\sigma}$ which we also write $\sigma = K|L$.

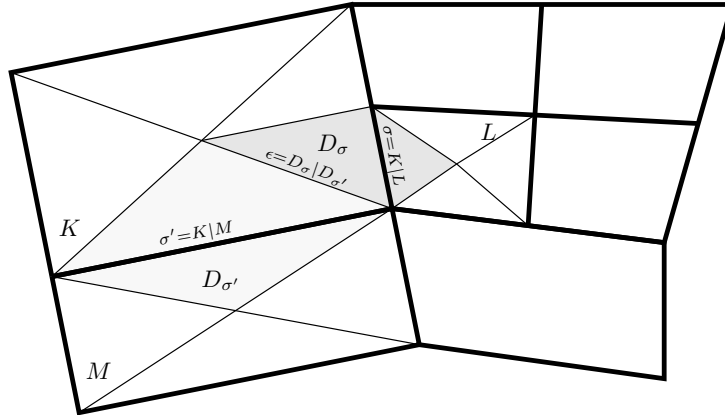


Figure 1. Notations for control volumes and diamond cells.

- $\mathcal{P} = (\mathbf{x}_K)_{K \in \mathcal{M}}$ is a set of points of Ω such that, $\forall K \in \mathcal{M}$, $\mathbf{x}_K \in K$.

We will need hereafter the following definitions. The normal vector to a face σ of K outward K is denoted by $\mathbf{n}_{K,\sigma}$, and \mathbf{x}_σ stands for the mass centre of the face σ . For any $K \in \mathcal{M}$ and any cell L sharing a face $K|L$ with K , we define the volume $D_{K,K|L}$ as the cone with basis $K|L$ and vertex \mathbf{x}_K . For $K \in \mathcal{M}$ and $\sigma \in \mathcal{E}$, we denote by $|K|$ the measure of K and by $|\sigma|$ the $(d-1)$ -measure of the face σ (see Figure 1).

Finally, for the time discretization, we will use a constant time step, denoted by δt , and we define $t^n = n \delta t$, for $0 \leq n \leq N = T/\delta t$.

3. The scheme

The discretization of (1) is performed by a first-order Euler scheme. It combines an explicit discretization of the convection operator and an implicit discretization of the diffusion term. Denoting by $u^n = (u_K^n)_{K \in \mathcal{M}}$ the discrete unknowns at time t^n , $1 \leq n \leq N$, the scheme reads:

for $0 \leq n \leq N-1$, $\forall K \in \mathcal{M}$,

$$\frac{|K|}{\delta t} (u_K^{n+1} - u_K^n) + \sum_{\sigma \in \mathcal{E}(K)} F_{K,\sigma} u_\sigma^n - \kappa |K| (\Delta_{\mathcal{M}} u^{n+1})_K = \frac{1}{\delta t} \int_{t^n}^{t^{n+1}} \int_K f(\mathbf{x}, t) \, d\mathbf{x} \, dt, \quad (2)$$

with, for $K \in \mathcal{M}$ and $\sigma \in \mathcal{E}(K)$:

$$u_K^0 = \frac{1}{|K|} \int_K u_0(\mathbf{x}) \, d\mathbf{x}, \quad F_{K,\sigma} = \frac{1}{\delta t} \int_{t^n}^{t^{n+1}} \int_\sigma \mathbf{v}(\mathbf{x}, t) \cdot \mathbf{n}_{K,\sigma} \, d\gamma(\mathbf{x}).$$

Note that, since \mathbf{v} is divergence free, we get:

$$\forall K \in \mathcal{M}, \quad \sum_{\sigma \in \mathcal{E}(K)} F_{K,\sigma} = 0. \quad (3)$$

The next two subsections are devoted to the description of the discrete diffusion operator ($\Delta_{\mathcal{M}} u^{n+1}$ in (2)) and the discrete convection term, which consists in the choice of the value of u_{σ}^n in (2).

3.1. Discretization of the diffusion operator

The idea for the discretization of the diffusion operator is related to that of the Galerkin methods; dropping for readability reasons the exponent $n + 1$ referring to time, it consists in exploiting an expression of the form:

$$(-\Delta_{\mathcal{M}} u)_K = \frac{1}{|K|} \left[\int_{\Omega} \nabla_{\mathcal{M}} u \cdot \nabla_{\mathcal{M}} \mathbf{1}^K - \int_{\partial\Omega_{\text{N}}} g_{\text{N}} \mathbf{1}^K \right], \quad (4)$$

where g_{N} stands for the flux at the Neumann boundary, $\mathbf{1}^K$ is a characteristic function associated to the cell K and $\nabla_{\mathcal{M}}$ denotes an *ad hoc* discrete gradient operator, which we define in this section.

We start by choosing, for any internal $\sigma \in \mathcal{E}_{\text{int}}$ and any face of the Neumann boundary $\sigma \in \mathcal{E}_{\text{N}}$, some real coefficients $(\beta_{\sigma}^L)_{L \in \mathcal{M}}$ such that the mass centre \mathbf{x}_{σ} of σ is expressed by:

$$\mathbf{x}_{\sigma} = \sum_{K \in \mathcal{M}} \beta_{\sigma}^K \mathbf{x}_K, \quad \sum_{K \in \mathcal{M}} \beta_{\sigma}^K = 1. \quad (5)$$

Note that it is always possible to restrict the number of nonzero coefficients β_{σ}^K to three in two space dimensions and to four in three space dimensions. In practice, we also try to avoid large variations of their values. To this purpose, for an internal edge $\sigma = K|L$, we give nonzero values to the coefficients associated to K and L , and then choose among the neighbours of K and L first those which lead to a set of positive coefficients (if any, which seems to be almost always the case in practice), then, among the possible sets, the one which corresponds to $\beta_{\sigma}^K + \beta_{\sigma}^L$ closest to one. For external edges, it is generally not possible to avoid negative coefficients.

We then introduce a second order interpolation operator of a discrete function at the points $(\mathbf{x}_{\sigma})_{\sigma \in \mathcal{E}}$. In usual finite element formulations, the Dirichlet boundary conditions are incorporated in the definition of the discrete space; here, since the unknowns are piecewise constant, the analogous effect is obtained by taking Dirichlet boundary conditions into account in the definition of the interpolation operator. This latter thus acts on a set larger than the cell values, which we call a discrete family, and which is defined as the union of cell values and values at the mass centres of the Dirichlet edges: $w_{\mathcal{M}} = ((w_K)_{K \in \mathcal{M}}, (w_{\text{D},\sigma})_{\sigma \in \mathcal{E}_{\text{D}}})$. Then the interpolate of the family $w_{\mathcal{M}}$ is defined by the data of its values at every face of the mesh $(w_{\sigma})_{\sigma \in \mathcal{E}}$:

$$\left| \begin{array}{ll} \forall \sigma \in \mathcal{E}_{\text{int}} \cup \mathcal{E}_{\text{N}}, & w_{\sigma} = \sum_{K \in \mathcal{M}} \beta_{\sigma}^K w_K, \\ \forall \sigma \in \mathcal{E}_{\text{D}}, & w_{\sigma} = w_{\text{D},\sigma}. \end{array} \right. \quad (6)$$

We may then introduce, for any discrete family $w_{\mathcal{M}}$, a first gradient $\overline{\nabla}w_{\mathcal{M}}$, defined by its constant value $(\overline{\nabla}w_{\mathcal{M}})_K$ on each cell K :

$$\forall K \in \mathcal{M}, \quad (\overline{\nabla}w_{\mathcal{M}})_K = \frac{1}{|K|} \sum_{\sigma \in \mathcal{E}(K)} |\sigma| (w_{\sigma} - w_K) \mathbf{n}_{K,\sigma}. \quad (7)$$

The discrete gradient thus defined is consistent, thanks to the following geometrical identity:

$$\forall K \in \mathcal{M}, \quad \sum_{\sigma \in \mathcal{E}(K)} |\sigma| \mathbf{n}_{K,\sigma} (\mathbf{x}_{\sigma} - \mathbf{x}_K)^t = |K| \mathbf{I}. \quad (8)$$

Indeed, let ψ be an affine function: $\mathbf{x} \mapsto \mathbf{a} \cdot \mathbf{x} + \mathbf{b}$, with $\mathbf{a}, \mathbf{b} \in \mathbb{R}^d$ (so that $\nabla\psi = \mathbf{a}$). Let $\psi_{\mathcal{M}}$ be the discrete family defined by $\psi_K = \psi(\mathbf{x}_K)$ for $K \in \mathcal{M}$ and $\psi_{\mathcal{D},\sigma} = \psi(\mathbf{x}_{\sigma})$ for any $\sigma \in \mathcal{E}_{\mathcal{D}}$, and let $\overline{\nabla}\psi_{\mathcal{M}}$ denote its discrete gradient defined by (7). Since ψ is affine, by definition of a second order interpolation, we have $\psi_{\sigma} - \psi_K = \psi(\mathbf{x}_{\sigma}) - \psi(\mathbf{x}_K) = \mathbf{a} \cdot (\mathbf{x}_{\sigma} - \mathbf{x}_K)$. Therefore:

$$(\overline{\nabla}\psi_{\mathcal{M}})_K = \frac{1}{|K|} \sum_{\sigma \in \mathcal{E}_K} |\sigma| \mathbf{a} \cdot (\mathbf{x}_{\sigma} - \mathbf{x}_K) \mathbf{n}_{K,\sigma} = \mathbf{a},$$

thanks to (8), and the discrete gradient of the interpolate of an affine function is equal to its exact gradient.

Unfortunately, this is not sufficient to ensure the convergence of the scheme. We also need a weak convergence property (see [9]) and a stability property which is not satisfied by the above gradient: indeed, as noted in [9] and illustrated in [6] in the case of Cartesian grids, this discrete gradient may vanish for non zero functions. We are thus lead to introduce the following stabilization term, defined for any discrete family $w_{\mathcal{M}}$ by:

$$\forall K \in \mathcal{M}, \quad \forall \sigma \in \mathcal{E}(K), \quad (Rw_{\mathcal{M}})_{K,\sigma} = \frac{\sqrt{d}}{d(\mathbf{x}_K, \sigma)} [w_{\sigma} - w_K - (\overline{\nabla}w)_{K,\sigma} \cdot (\mathbf{x}_{\sigma} - \mathbf{x}_K)], \quad (9)$$

where $d(\mathbf{x}_K, \sigma)$ stands for the distance of \mathbf{x}_K to σ . Note that $(Rw_{\mathcal{M}})_{K,\sigma}$ vanishes if $w_{\mathcal{M}}$ is the interpolate of an affine function; the quantity $(Rw_{\mathcal{M}})_{K,\sigma}$ thus may be seen as a consistency error on the half-diamond cell $D_{K,\sigma}$.

We then define the discrete gradient of a family $w_{\mathcal{M}}$ as the piecewise constant function on the half-diamond cells $D_{K,\sigma}$ defined by:

$$(\nabla w_{\mathcal{M}})_{K,\sigma} = (\overline{\nabla}w_{\mathcal{M}})_K + (Rw_{\mathcal{M}})_{K,\sigma} \mathbf{n}_{K,\sigma}, \quad \text{on } D_{K,\sigma}. \quad (10)$$

We can now define the diffusion term $(-\Delta_{\mathcal{M}}u)_K$, for $K \in \mathcal{M}$. To the unknown u , we associate the discrete family $u_{\mathcal{M}} = ((u_K)_{K \in \mathcal{M}}, (u_{\mathcal{D},\sigma})_{\sigma \in \mathcal{E}_{\mathcal{D}}})$, where $u_{\mathcal{D},\sigma}$ stands for the mean value over the face σ of the Dirichlet condition $\bar{\mathbf{u}}_{\mathcal{D}}$. Then we define $\mathbf{1}^K$ as the discrete family defined by $(\mathbf{1}^K)_K = 1$, $(\mathbf{1}^K)_L = 0$ for any cell $L \neq K$, and $(\mathbf{1}^K)_{\mathcal{D},\sigma} = 0$, $\forall \sigma \in \mathcal{E}_{\mathcal{D}}$. The value of $(-\Delta_{\mathcal{M}}u)_K$ is then given by (4), with the definition (10) of the discrete gradient, thus, specifying the domains of integration:

$$(-\Delta_{\mathcal{M}}u)_K = \frac{1}{|K|} \left[\sum_{L \in \mathcal{M}} \sum_{\sigma \in \mathcal{E}(L)} |D_{L,\sigma}| (\nabla u_{\mathcal{M}})_{L,\sigma} \cdot (\nabla \mathbf{1}^K)_{L,\sigma} - \sum_{\sigma \in \mathcal{E}_{\mathcal{N}}} (\mathbf{1}^K)_{\sigma} \int_{\sigma} g_{\mathcal{N}} \right],$$

where $(\mathbf{1}^K)_{\sigma}$ is given by (6).

Remark 1 (Consistency with the two-point scheme and maximum principle)

If one only wants to ensure the stability of the scheme, the quantity $(Ru_{\mathcal{M}})_{K,\sigma}$ is defined up to a multiplicative constant; indeed the specific coefficient \sqrt{d} in (9) is chosen so as to recover the usual finite volume two-point diffusion flux for (2D) acute angle triangular meshes and for rectangular grids ($d = 2$ or $d = 3$), provided that the choice for the points $(\mathbf{x}_K)_{K \in \mathcal{M}}$ is the usual one, namely the circumcenter of the triangle K in the first case and the mass centre of K in the second one [9, Lemma 2.1].

In this case, the proposed discretization of the diffusion term thus satisfies a discrete maximum principle, which does not hold in the general case, as stated in Theorem 3.2.

Remark 2 (Extension to variable diffusion coefficient) The extension of the scheme to variable diffusion coefficient may be done by defining a diffusion coefficient κ_K , for $K \in \mathcal{M}$, and changing (4) to:

$$((-\operatorname{div} \kappa \nabla)_{\mathcal{M}} u)_K = \frac{1}{|K|} \left[\int_{\Omega} \kappa_K \nabla_{\mathcal{M}} u \cdot \nabla_{\mathcal{M}} \mathbf{1}^K - \int_{\partial\Omega_N} g_N \mathbf{1}^K \right].$$

The result of Remark 1 then still holds, with an expression of the (two-point) flux involving a diffusion at the face which is identical to the classical harmonic average under geometrical conditions on the mesh (see [9, Lemma 2.1] for the expression of the diffusion coefficient).

Remark 3 (The interpolate of the functions $\mathbf{1}^K$ in 1D)

For the sake of clarity, we illustrate the construction of the interface values. Let us suppose that we work on the one-dimensional domain $\Omega = (0, 1)$, with a constant space step. We suppose in addition that the solution is prescribed at $\mathbf{x} = 0$ and obeys a Neumann boundary condition at $\mathbf{x} = 1$, so that we have to provide a way to calculate an interpolated value of discrete families at any internal interface and at the interface located at $\mathbf{x} = 1$. To this purpose, a reasonable choice seems to be the following one:

- at an internal face, the interpolated value is defined as the average of the values taken at the two neighbouring cells,
- at the interface σ located at $\mathbf{x} = 1$, we set:

$$u_{\sigma} = \frac{3}{2} u_{K_N} - \frac{1}{2} u_{K_{N-1}},$$

where N stands for the number of cells, and the cells are indexed from $\mathbf{x} = 0$ to $\mathbf{x} = 1$.

The interpolated values obtained with this choice for the characteristic function of the cells of the mesh are given on Figure 2.

3.2. Discretization of the convection operator

The strategy used to design the convection scheme relies on the following remark: it is possible to state some conditions for the values u_{σ}^n of the unknown at the face which are sufficient to ensure that the scheme satisfies a discrete maximum principle (in a sense given by Lemma 3.1 then Theorem 3.2 below); moreover, these conditions provide an admissible interval for the (u_{σ}^n) . Then a discretization naturally follows: first compute a tentative value for (u_{σ}^n) by an affine interpolation, and then "limit the flux" (according to the terminology of the MUSCL family of schemes) by projecting this value on the admissible interval.

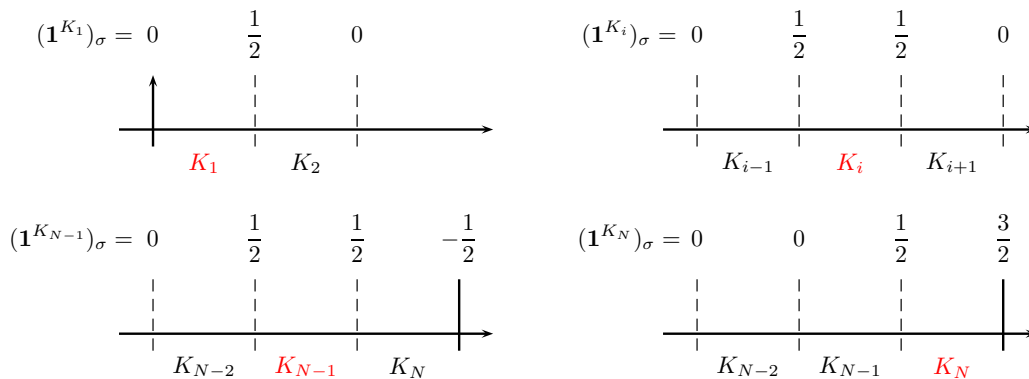


Figure 2. Interpolated values for the characteristic functions of the cells in 1D.

The present exposition follows this line: we first state the conditions to be satisfied by the face values (Section 3.2.1), then show how they may be exploited to obtain a limitation procedure (Section 3.2.2).

3.2.1. Conditions for the satisfaction of a maximum principle The usual first order scheme for the convection operator is the upstream scheme, which consists in choosing u_σ^n in (2) for an internal face $\sigma = K|L$ as follows:

$$u_\sigma^n = u_K \text{ if } F_{K,\sigma} \geq 0, \quad u_\sigma^n = u_L \text{ otherwise.} \quad (11)$$

The upstream choice is wellknown to ensure the maximum principle. Let us briefly review the ingredients which yield this property. For $K \in \mathcal{M}$, let \tilde{u}_K^{n+1} stand for the value updated with the convection term:

$$\tilde{u}_K^{n+1} = u_K^n - \frac{\delta t}{K} \sum_{\sigma \in \mathcal{E}(K)} F_{K,\sigma} u_\sigma^n. \quad (12)$$

Using the discrete divergence-free constraint (3), with u_σ^n defined by (11), we get:

$$\tilde{u}_K^{n+1} = \left[1 - \frac{\delta t}{K} \sum_{\sigma \in \mathcal{E}(K)} \max(F_{K,\sigma}, 0) \right] u_K^n - \frac{\delta t}{K} \sum_{\sigma \in \mathcal{E}(K), \sigma = K|L} \min(F_{K,\sigma}, 0) u_L^n. \quad (13)$$

We denote by cfl the following number:

$$\text{cfl} = \max_{K \in \mathcal{M}} \left\{ \frac{1}{|K|} \sum_{\sigma \in \mathcal{E}(K)} |F_{K,\sigma}| \right\}. \quad (14)$$

Then, under the so-called CFL-condition $\text{cfl} \leq 1$, Equation (13) yields that \tilde{u}_K^{n+1} is a convex combination of the values taken by u^n in the neighbouring cells of K .

The same principle holds for MUSCL-type schemes which attempt to go higher order while remaining stable: a piecewise linear reconstruction is performed to evaluate the quantities

u_σ^n , and the resulting slopes are limited in order for the expression (12) to remain a convex combination of the values taken by u^n in the neighbouring cells of K . For a linear advection term such as addressed here, this latter property is shown to be ensured by the following conditions. First, for internal faces, we suppose:

$\forall K \in \mathcal{M}, \forall \sigma \in \mathcal{E}(K) \cap \mathcal{E}_{\text{int}}$, there exists $\alpha_\sigma^K \in [0, 1]$ and a cell $M_\sigma^K \in \mathcal{M}$ such that

$$u_\sigma^n - u_K^n = \begin{cases} \alpha_\sigma^K (u_K - u_{M_\sigma^K}) & \text{if } F_{K,\sigma} \geq 0 \\ \alpha_\sigma^K (u_{M_\sigma^K} - u_K) & \text{otherwise.} \end{cases} \quad (15)$$

Then, we denote by \mathcal{E}_D^- (resp. \mathcal{E}_D^+) the faces σ of \mathcal{E}_D where the flow is entering (resp. leaving) the domain, *i.e.* $F_{K,\sigma} \leq 0$ (resp. $F_{K,\sigma} \geq 0$). For the faces included in \mathcal{E}_D^+ and \mathcal{E}_N (where, by assumption $F_{K,\sigma} \geq 0$), we suppose that the (first part of) (15) holds. For faces of \mathcal{E}_D^- , we suppose that u_σ^n is given by the boundary conditions, which we denote by $u_\sigma^n = u_{D,\sigma}^n$.

The obtained stability property is stated below and its proof is recalled for the sake of completeness.

Lemma 3.1. *Let us suppose that $\text{cfl} \leq 1$. Let $K \in \mathcal{M}$. We denote by $\mathcal{N}_m(K)$ the set of cells M_σ^K , $\sigma \in \mathcal{E}(K)$, which are such that (15) is satisfied. Then, $\forall K \in \mathcal{M}$, the value \tilde{u}_K^{n+1} given by (12) is a convex combination of $\{u_K^n, (u_M^n)_{M \in \mathcal{N}_m(K)}, (u_{D,\sigma}^n)_{\sigma \in \mathcal{E}_D^- \cap \mathcal{E}(K)}\}$.*

Proof Let $K \in \mathcal{M}$. By definition, we get:

$$\frac{|K|}{\delta t} \tilde{u}_K^{n+1} = \frac{|K|}{\delta t} u_K^n - \sum_{\sigma \in \mathcal{E}(K)} F_{K,\sigma} u_\sigma^n,$$

and thus, invoking as above the discrete divergence-free constraint (3):

$$\frac{|K|}{\delta t} \tilde{u}_K^{n+1} = \frac{|K|}{\delta t} u_K^n - \sum_{\sigma \in \mathcal{E}(K)} F_{K,\sigma}^+ (u_\sigma^n - u_K^n) + \sum_{\sigma \in \mathcal{E}(K)} F_{K,\sigma}^- (u_\sigma^n - u_K^n).$$

Let us first consider the internal faces where the flow is entering K , *i.e.* $F_{K,\sigma}^- \geq 0$, $F_{K,\sigma}^+ = 0$. By (15), there exists a cell $M_\sigma \in \mathcal{N}_\sigma(K)$ and $\alpha_\sigma \in [0, 1]$ such that:

$$u_\sigma^n - u_K^n = \alpha_\sigma (u_{M_\sigma}^n - u_K^n), \quad \text{so} \quad F_{K,\sigma}^- (u_\sigma^n - u_K^n) = \alpha_\sigma F_{K,\sigma}^- (u_{M_\sigma}^n - u_K^n).$$

Similarly, on the faces (including faces of \mathcal{E}_N and \mathcal{E}_D^+) where the flow is leaving K , *i.e.* $F_{K,\sigma}^+ \geq 0$, $F_{K,\sigma}^- = 0$, by (15), there exists $M_\sigma \in \mathcal{N}_\sigma(K)$ and $\alpha_\sigma \in [0, 1]$ such that:

$$u_\sigma^n - u_K^n = \alpha_\sigma (u_K^n - u_{M_\sigma}^n), \quad \text{so} \quad -F_{K,\sigma}^+ (u_\sigma^n - u_K^n) = \alpha_\sigma F_{K,\sigma}^+ (u_{M_\sigma}^n - u_K^n).$$

With these expressions, we thus get:

$$\begin{aligned} \frac{|K|}{\delta t} \tilde{u}_K^{n+1} &= \left[\frac{|K|}{\delta t} - \sum_{\sigma \in \mathcal{E}(K) \setminus \mathcal{E}_D} \alpha_\sigma |F_{K,\sigma}| - \sum_{\sigma \in \mathcal{E}(K) \cap \mathcal{E}_D} F_{K,\sigma}^- \right] u_K^n \\ &+ \sum_{\sigma \in \mathcal{E}(K) \setminus \mathcal{E}_D} \alpha_\sigma |F_{K,\sigma}| u_{M_\sigma}^n + \sum_{\sigma \in \mathcal{E}(K) \cap \mathcal{E}_D^-} F_{K,\sigma}^- u_{D,\sigma}^n, \end{aligned}$$

which concludes the proof, since $\text{cfl} \leq 1$. \blacksquare

For the sake of thoroughness, we now show that, under assumptions on the diffusion operator, this result yields a discrete maximum principle for the complete scheme (2). To this purpose, let us write (2) as:

$$\left((\text{Id} - \kappa \delta t \Delta_{\mathcal{M}}) u^{n+1} \right)_K = \tilde{u}_K^{n+1}, \quad (16)$$

where $\text{Id} - \kappa \delta t \Delta_{\mathcal{M}}$ stands for the operator acting on discrete functions which maps $u = (u_K)_{K \in \mathcal{M}}$ to $(\text{Id} - \kappa \delta t \Delta_{\mathcal{M}}) u = (u_K - \kappa \delta t (\Delta_{\mathcal{M}} u)_K)_{K \in \mathcal{M}}$. Note that, from the definition of the discrete Laplace operator of Section 3.1, this operator is affine, and not linear (*i.e.*, in the case of non-homogeneous Dirichlet boundary conditions, $(\text{Id} - \kappa \delta t \Delta_{\mathcal{M}}) u$ does not vanish for $u = 0$).

Theorem 3.2 (A discrete maximum principle)

Let us suppose that $\text{cfl} \leq 1$, and that both $f = 0$ and $g_{\mathcal{N}} = 0$. Then we have the following stability results:

- (i) if $\kappa = 0$, the solution to the scheme (2) satisfies a local maximum principle, namely $\forall K \in \mathcal{M}$, u_K^{n+1} is a convex combination of $\{u_K^n, (u_M^n)_{M \in \mathcal{N}_m(K)}, (u_{\mathcal{D}, \sigma}^n)_{\sigma \in \mathcal{E}_{\mathcal{D}}^- \cap \mathcal{E}(K)}\}$.
- (ii) if the discrete Laplace operator is such that:
 - (ii - a) for any constant function u such that $u \leq \min \{(u_{\mathcal{D}, \sigma})_{\sigma \in \mathcal{E}_{\mathcal{D}}}\}$ (*resp.* $u \geq \max \{(u_{\mathcal{D}, \sigma})_{\sigma \in \mathcal{E}_{\mathcal{D}}}\}$), $-\Delta_{\mathcal{M}} u \leq 0$ (*resp.* $-\Delta_{\mathcal{M}} u \geq 0$),
 - (ii - b) all the entries of the inverse of the matrix $M_{I - \kappa \delta t \Delta}$ associated to the operator $\text{Id} - \kappa \delta t \Delta_{\mathcal{M}}$ are non-negative, *i.e.* $M_{I - \kappa \delta t \Delta}$ is a positive inverse matrix.

the solution to the scheme (2) satisfies the following global maximum principle:

$$\begin{aligned} \forall K \in \mathcal{M}, \quad \min \left\{ (u_M^n)_{M \in \mathcal{M}}, (u_{\mathcal{D}, \sigma}^n)_{\sigma \in \mathcal{E}_{\mathcal{D}}^-}, (u_{\mathcal{D}, \sigma}^{n+1})_{\sigma \in \mathcal{E}_{\mathcal{D}}} \right\} &\leq u_K^{n+1} \\ &\leq \max \left\{ (u_M^n)_{M \in \mathcal{M}}, (u_{\mathcal{D}, \sigma}^n)_{\sigma \in \mathcal{E}_{\mathcal{D}}^-}, (u_{\mathcal{D}, \sigma}^{n+1})_{\sigma \in \mathcal{E}_{\mathcal{D}}} \right\}. \end{aligned}$$

Proof When $\kappa = 0$, the scheme (2) (or (16)) boils down to $\tilde{u}_K^{n+1} = u_K^{n+1}$, $\forall K \in \mathcal{M}$, Item (i) is a straightforward consequence of Lemma 3.1. We now turn to Item (ii) and define \underline{u} by:

$$\underline{u} = \min \left\{ (u_K^n)_{K \in \mathcal{M}}, (u_{\mathcal{D}, \sigma}^n)_{\sigma \in \mathcal{E}_{\mathcal{D}}^-}, (u_{\mathcal{D}, \sigma}^{n+1})_{\sigma \in \mathcal{E}_{\mathcal{D}}} \right\}.$$

We have, $\forall K \in \mathcal{M}$:

$$\left((\text{Id} - \kappa \delta t \Delta_{\mathcal{M}}) (u^{n+1} - \underline{u}) \right)_K = \tilde{u}_K^{n+1} - \underline{u}^n + \kappa \delta t (\Delta_{\mathcal{M}} \underline{u})_K. \quad (17)$$

By Lemma 3.1 and Assumption (ii - a), the right-hand side of this relation is non-negative, which, since, by Assumption (ii - b), the operator at the left-hand side is associated to a positive inverse matrix, yields that $u^{n+1} - \underline{u}$ is non-negative. The other estimate follows by the same computation with $\underline{u} = \max \{(u_K^n)_{K \in \mathcal{M}}, (u_{\mathcal{D}, \sigma}^n)_{\sigma \in \mathcal{E}_{\mathcal{D}}^-}, (u_{\mathcal{D}, \sigma}^{n+1})_{\sigma \in \mathcal{E}_{\mathcal{D}}}\}$. \blacksquare

Remark 4. Assumptions (ii - a) and (ii - b) are satisfied with the usual two-point-flux finite volume operator; unfortunately, this is not the case for the discrete Laplace operator introduced in Section 3.1 (neither, to our knowledge, by any linear discrete diffusion operator acting on general meshes).

3.2.2. A limitation procedure, and the convection scheme We now reformulate (15) to obtain a limitation procedure, *i.e.* a constructive process to bound the face values u_σ^n .

Let $\sigma \in \mathcal{E}_{\text{int}}$, let us denote by V^- and V^+ the upstream and downstream cell separated by σ , and by $\mathcal{N}_\sigma(V^-)$ and $\mathcal{N}_\sigma(V^+)$ two sets of neighbouring cells of V^- and V^+ respectively. We would like to use (15), or possibly a stronger version of (15), to define an admissible interval for u_σ^n ; this admissible interval must allow the usual upstream choice, *i.e.* $u_\sigma^n = u_{V^-}^n$. This is realized by the following two assumptions, provided that $V^- \in \mathcal{N}_\sigma(V^+)$ (see Remark 5), which we thus suppose:

$$(H1) - \text{ there exists } M \in \mathcal{N}_\sigma(V^+) \text{ such that } u_\sigma^n \in \llbracket u_M^n, u_M^n + \frac{\zeta^+}{2}(u_{V^+}^n - u_M^n) \rrbracket,$$

$$(H2) - \text{ there exists } M \in \mathcal{N}_\sigma(V^-) \text{ such that } u_\sigma^n \in \llbracket u_{V^-}^n, u_{V^-}^n + \frac{\zeta^-}{2}(u_{V^-}^n - u_M^n) \rrbracket,$$

where, for $a, b \in \mathbb{R}$, we denote by $\llbracket a, b \rrbracket$ the interval $\{\alpha a + (1 - \alpha)b, \alpha \in [0, 1]\}$, and ζ^+ and ζ^- are two numerical parameters lying in the interval $[0, 2]$. For $\sigma \in \mathcal{E}_N \cup \mathcal{E}_D^+$, Condition (H1) is irrelevant, and the only acting constraint is Condition (H2). The sets $\mathcal{N}_\sigma(V^-)$ and $\mathcal{N}_\sigma(V^+)$ have to be specified to complete the definition of the limitation process.

The link between (H1)-(H2) and (15) is quite obvious, as we now show. Let $K \in \mathcal{M}$ and $\sigma \in \mathcal{E}(K)$. If $F_{K,\sigma} \leq 0$, *i.e.* K is the downstream cell for σ denoted above by V^+ , since $\zeta^+ \in [0, 2]$, condition (H1) yields that there exists $M \in \mathcal{M}$ such that $u_\sigma^n \in \llbracket u_K^n, u_M^n \rrbracket$ which is (15). Otherwise, *i.e.* if $F_{K,\sigma} \geq 0$ and K is the upstream cell for σ denoted above by V^- , condition (H2) yields that there exists $M \in \mathcal{M}$ such that $u_\sigma^n \in \llbracket u_K^n, 2u_K^n - u_M^n \rrbracket$, so $u_\sigma^n - u_K^n \in \llbracket 0, u_K^n - u_M^n \rrbracket$, which is once again (15).

Remark 5. For $\sigma \in \mathcal{E}_{\text{int}}$, since $V^- \in \mathcal{N}_\sigma(V^+)$, the upstream choice $u_\sigma^n = u_{V^-}^n$ always satisfies the conditions (H1) and (H2), and is the only one to satisfy them if we choose $\zeta^- = \zeta^+ = 0$.

Remark 6 (1D case) Let us take the example of an edge σ separating K_i and K_{i+1} in a 1D case (see Figure 3 for the notations), with a uniform meshing and a positive advection velocity, so that $V^- = K_i$ and $V^+ = K_{i+1}$. In 1D, a natural choice is $\mathcal{N}_\sigma(K_i) = \{K_{i-1}\}$ and $\mathcal{N}_\sigma(K_{i+1}) = \{K_i\}$.

On Figure 3, we sketch: on the left, the admissible interval given by (H1) with $\zeta^+ = 1$ (green) and $\zeta^+ = 2$ (orange); on the right, the admissible interval given by (H2) with $\zeta^- = 1$ (green) and $\zeta^- = 2$ (orange). The parameters ζ^- and ζ^+ may be seen as limiting the admissible slope between (\mathbf{x}_i, u_i^n) and $(\mathbf{x}_\sigma, u_\sigma^n)$ (with \mathbf{x}_i the abscissa of the mass centre of K_i and \mathbf{x}_σ the abscissa of σ), with respect to a left and right slope, respectively. For $\zeta^- = \zeta^+ = 1$, one recognises the usual minmod limiter (*eg.* [11, Chapter III]).

Note that, since, on the example depicted on Figure 3, the discrete function u^n has an extremum in K_i , the combination of the conditions (H1) and (H2) imposes that, as usual, the only admissible value for u_σ^n is the upwind one.

We are now in position to give the algorithm used for the discretization of the convection term:

1. Compute a tentative value \tilde{u}_σ for the unknown at the face σ , by Relation (6), which yields an affine interpolation at the mass centre of the face.

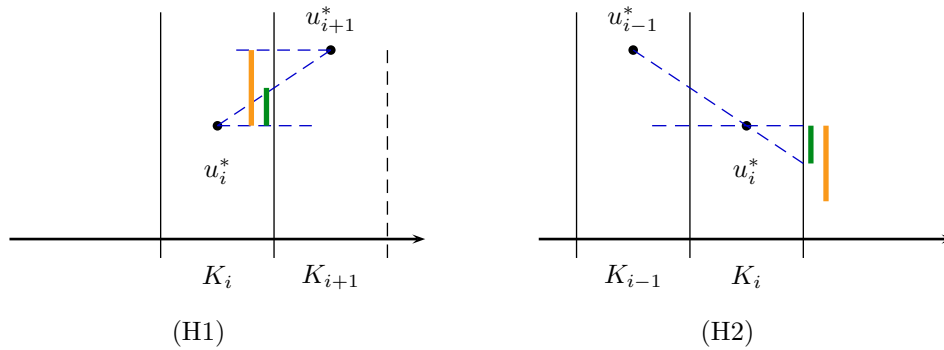
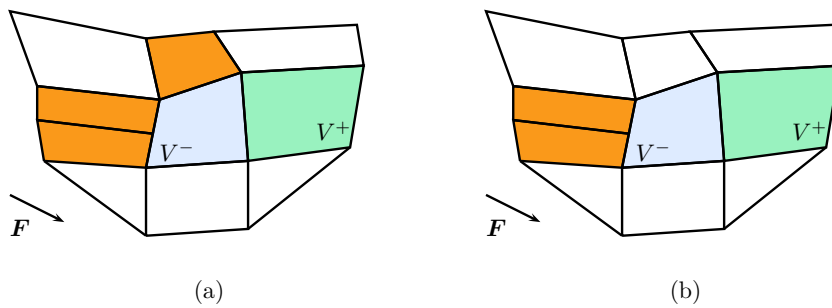


Figure 3. Conditions (H1) and (H2) in 1D.

Figure 4. Notations for the definition of the limitation process. In orange, control volumes of the set $\mathcal{N}_\sigma(V^-)$ for $\sigma = V^-|V^+$, with a constant advection field \mathbf{F} : upwind cells (a) or opposite cells (b).

2. For each face σ of the mesh, determine V^- and V^+ according to the sign of the mass flux through σ , and exploit (H1) and (H2) to obtain an admissible interval I_σ for the value of the unknown at the face, which, as explained in Remark 5, is not empty.

This step depends on the definition of the sets $\mathcal{N}_\sigma(V^-)$ and $\mathcal{N}_\sigma(V^+)$. Here, we just set $\mathcal{N}_\sigma(V^+) = \{V^-\}$; note however that this choice prevents second order, since an affine function is not represented exactly (see Remark 7 below). Two different choices of $\mathcal{N}_\sigma(V^-)$ are implemented (see Figure 4):

- (a) $\mathcal{N}_\sigma(V^-)$ is defined as the set of "upstream cells" to V^- , *i.e.* $\mathcal{N}_\sigma(V^-) = \{L \in \mathcal{M}, L \text{ shares a face } \sigma \text{ with } V^- \text{ and } F_{V^-,\sigma} < 0\}$,
- (b) when this makes sense (*i.e.* with a mesh obtained by Q_1 mappings from the $(0,1)^d$ reference element), $\mathcal{N}_\sigma(V^-)$ may be chosen as the opposite cells to σ in V^- . Note that, for a structured mesh, this choice allows to recover the usual minmod limiter.

3. Compute u_σ as the nearest point to \tilde{u}_σ in I_σ .

Remark 7 (Reconstruction of affine functions) Let us suppose that we are trying to transport (*i.e.*, in fact, to keep constant) in \mathbb{R}^2 the initial function $u(\mathbf{x}) = \mathbf{x}_2$, with a constant

advection velocity $\mathbf{u} = (1, 0)^t$. Let K_1 and K_2 be two cells, of mass centre located at $\mathbf{x}_1 = (1, 0)^t$ and $\mathbf{x}_2 = (2, 0)^t$ respectively, and suppose that we initialize the scheme by setting for any $K \in \mathcal{M}$ the value u_K at the mean value of $u(\mathbf{x})$, so that $u_{K_1} = u_{K_2} = 0$. Let the face $\sigma = K_1|K_2$ be vertical, with a mass centre located at $\mathbf{x}_\sigma = (1.5, 0.5)^t$. Any affine reconstruction must yield $u_\sigma = u(\mathbf{x}_\sigma) = 0.5$ for the value u_σ of the approximation of u on σ , but Condition (H1) with $\mathcal{N}_\sigma(K_2) = \{K_1\}$ yields $u_\sigma = 0$.

4. Numerical tests

The computations performed in this section were performed with the open-source ISIS computer code [13], developed at IRSN on the basis of the software component library PELICANS [15].

4.1. Transport of irregular functions

We address the pure transport (*i.e.* without diffusion), of an irregular function defined on $\Omega = (-1, 1)^2$ as follows:

$$\begin{aligned} \text{for } \mathbf{x} \in (0.1, 0.6) \times (-0.25, 0.25), & \quad u = 1, \\ \text{if } r < 0.35, & \quad u = 1 - \frac{r}{0.35}, \\ \text{otherwise,} & \quad u = 0. \end{aligned}$$

where r stands for the distance from the current point \mathbf{x} to the point $(-0.45, 0)^t$, *i.e.* $r^2 = (\mathbf{x}_1 + 0.45)^2 + \mathbf{x}_2^2$. The advection field is given by $\mathbf{v}(\mathbf{x}) = 2(\mathbf{x}_2, -\mathbf{x}_1)^t$, so, at the end of n complete revolutions, the solution is identical to the initial condition for $t = n\pi$, $n \in \mathbb{N}$.

We begin with uniform Cartesian grids. If we set $\mathcal{N}_\sigma(V^-)$ to the opposite cell and choose $\zeta^+ = \zeta^- = 1$, the proposed scheme boils down to an usual MUSCL scheme with a minmod limiter (see Remark 6). Results obtained with a 120×120 mesh and $\delta t = \pi/(125 * n)$ (which yields a cfl number close to 1) at $t = \pi$ are plotted on Figure 5.

On Figure 6, we plot the value of the unknown along the x -axis, for the same mesh and time step and various options of the scheme: the MUSCL minmod one, the upwind scheme (obtained here by taking $\zeta^+ = \zeta^- = 0$), and two variants with less stringent limitations obtained by taking $\zeta^+ = \zeta^- = 2$ and by enlarging $\mathcal{N}_\sigma(V^-)$ to the set of upstream cells. At first glance, results may seem better with less limitation, but the shape of the initial condition is deformed, as may be seen on Figure 7.

We next turn to unstructured meshes. Starting from a regular Cartesian grid and applying a random displacement of length $0.3h$ to each node, we first obtain an unstructured quadrangular mesh; then, splitting each cell in four along its diagonals, we obtain a simplicial mesh. The coarsest meshes used in this study, together with the discrete initial condition (determined for each cell K as the value of the initial data at \mathbf{x}_K), are plotted on Figure 8. From now on, we restrict the choice for $\mathcal{N}_\sigma(V^-)$ to the opposite mesh for quadrangles and to the set of upstream cells for simplices, and we set $\zeta^+ = \zeta^- = 1$.

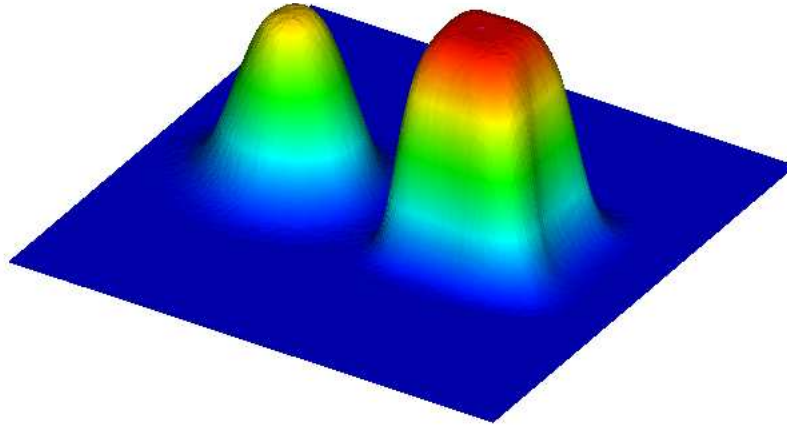


Figure 5. Transport of irregular functions - Results obtained with the usual MUSCL scheme and a minmod limiter, for a uniform 120×120 Cartesian grid.

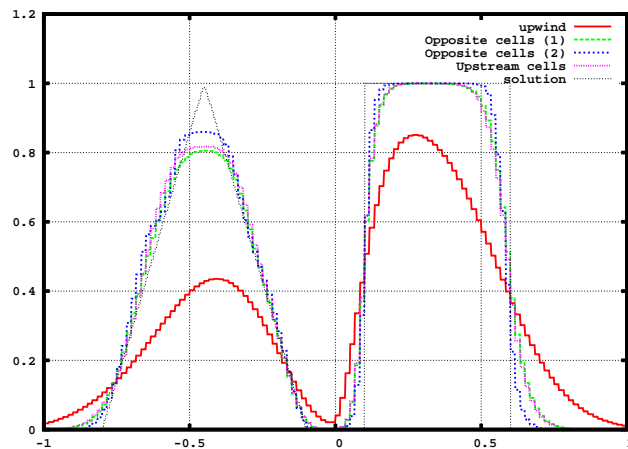


Figure 6. Transport of irregular functions - Value of the unknown along the x -axis obtained with the usual upwind scheme, the MUSCL minmod scheme (curve **Opposite cell (1)**), the same scheme with $\zeta^+ = \zeta^- = 2$ (curve **Opposite cell (2)**), and taking for $\mathcal{N}_\sigma(V^-)$ to the set of upstream cells, for a uniform 120×120 Cartesian grid.

The value of the unknown along the x -axis is plotted for meshes obtained from $n \times n$ structured grids, with $n = 20, 40, 80, 160$ and 320 , and $\delta t = \pi/(175 * n)$, for quadrangles (Figure 9) and $n = 20, 40, 80$ and 160 , and $\delta t = \pi/(600 * n)$, for triangles (Figure 10). In both cases, the cfl number is near to 1, and is the same for all the computations performed with the same family of meshes (*i.e.* quadrangular or simplicial meshes). The main qualitative effect of using an unstructured mesh seems to be an additional smearing of the solution.

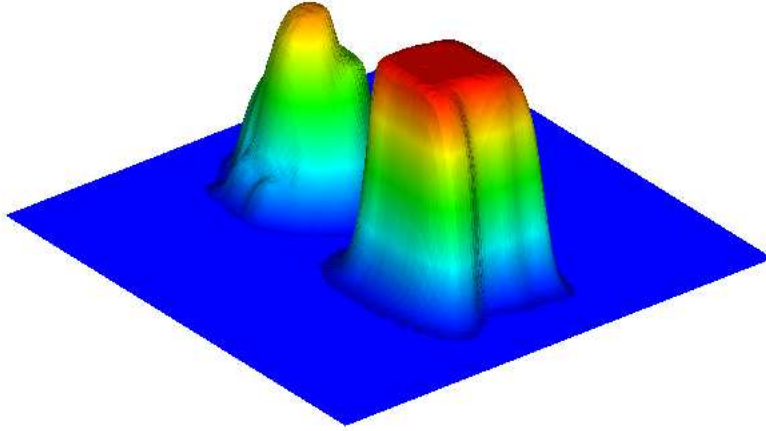


Figure 7. Transport of irregular functions - Results obtained with less limitation ($\zeta^+ = \zeta^- = 2$), for a uniform 120×120 Cartesian grid.

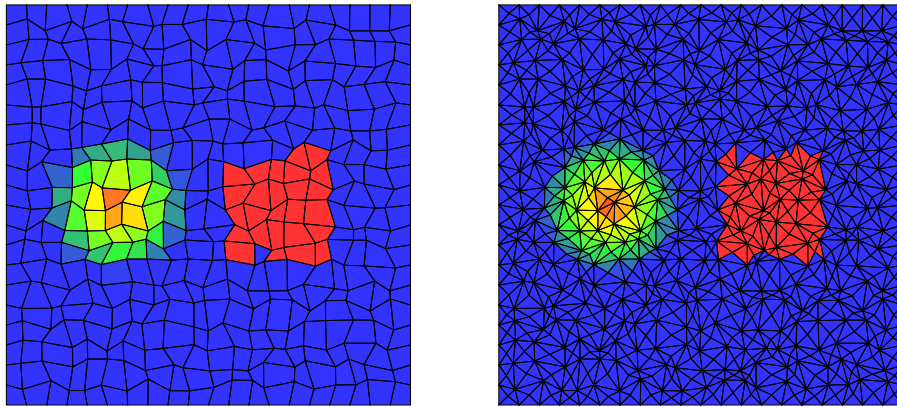


Figure 8. Transport of irregular functions - Mesh and initial value for quadrangular (left) and simplicial (right) meshes obtained from an initial 20×20 structured Cartesian grid.

The difference between the obtained solution, in a discrete L^1 -norm defined by:

$$\|u\|_{L^1, \mathcal{M}} = \sum_{K \in \mathcal{M}} |K| |u(\mathbf{x}_K)|,$$

is given in the following table, as a function of the initial regular grid, for the different computations already invoked in this study.

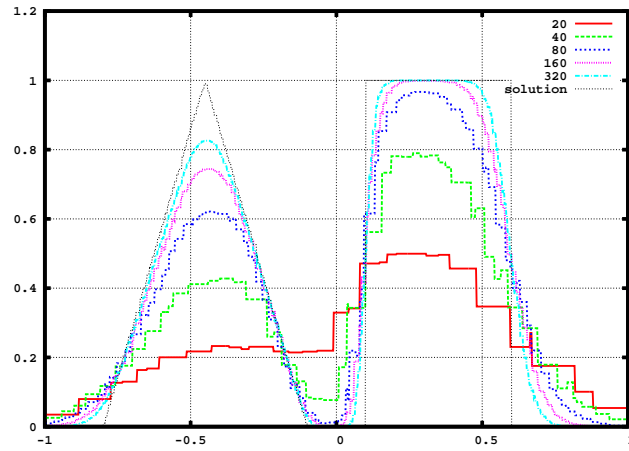


Figure 9. Transport of irregular functions - Value of the unknown along the x -axis, obtained with the quadrangular cells, as a function of the mesh step.

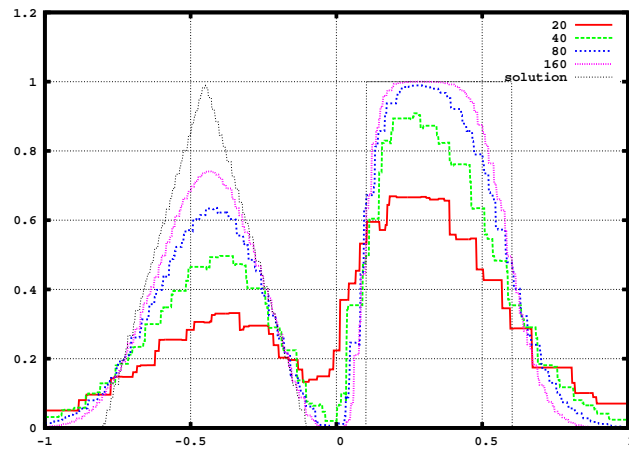


Figure 10. Transport of irregular functions - Value of the unknown along the x -axis, obtained with simplicial cells, as a function of the mesh step.

initial mesh	20×20	40×40	80×80	160×160	320×320
structured mesh	0.38	0.21	0.12	0.077	0.042
quadrangles	0.42	0.28	0.18	0.12	0.081
triangles	0.37	0.26	0.19	0.13	//

As may be expected, the accuracy is lower with unstructured meshes, and the fact that the numerical diffusion is greater is confirmed by the comparison of the trace of the solutions along

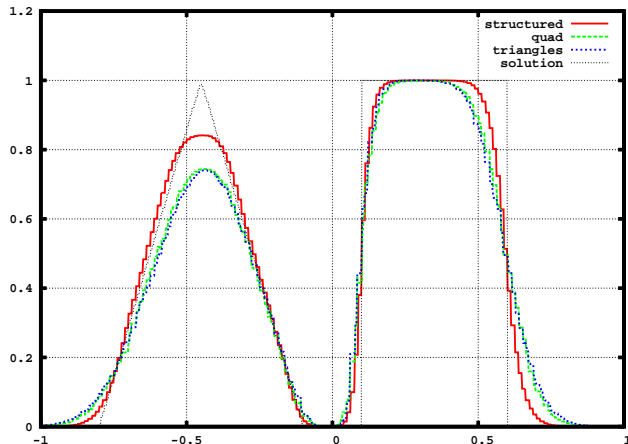


Figure 11. Transport of irregular functions - Value of the unknown along the x -axis, obtained with various meshes, built from a regular 160×160 mesh.

the line $x_2 = 0$ obtained with the various meshes built in this study from the 160×160 grid, displayed on Figure 11.

To conclude, we assess the capability of the scheme to deal with a locally refined non-conforming mesh. To this purpose, we start from a regular quadrangular mesh and split in four the cells located above the line $x_2 = 0$. Results obtained at $t = \pi$, starting with a 80×80 regular grid, are displayed on Figure 12 and Figure 13. No spurious numerical phenomenon is observed (especially near hanging nodes), and the computation performed with the partially refined mesh appears less diffusive. As predicted by the theory, here as in all the performed test cases, no overshoot or undershoot of the solution is observed (*i.e.*, here, the solution remains in the interval $[0, 1]$).

4.2. A convection-diffusion case

We now turn to a convection-diffusion tests case, built by combining a classical solution of the heat equation with a constant skew-to-the mesh transport. The computational domain is $\Omega = (0, 2) \times (0, 2)$, the advection velocity is $\mathbf{v} = (0.8, 0.8)^t$, the solution is given by:

$$u = \frac{1}{4t+1} \exp\left(\frac{X^2 + Y^2}{\kappa(4t+1)}\right), \quad \begin{bmatrix} X \\ Y \end{bmatrix} = \mathbf{x} - \left(\begin{bmatrix} 0.5 \\ 0.5 \end{bmatrix} + t \mathbf{v}\right),$$

with $\kappa = 0.01$. The function u satisfies the advection-diffusion equation (1a) with $f = 0$, and initial and Dirichlet boundary conditions given by value of u at $t = 0$ and on $\partial\Omega$ respectively.

As in the previous section, we use meshes of quadrangles obtained by perturbation of regular grids, by a displacement of each node in a random direction, here of length $0.2h$. We reduce $\mathcal{N}_\sigma(V^-)$ to the opposite mesh of σ in V^- and choose $\zeta^+ = \zeta^- = 1$.

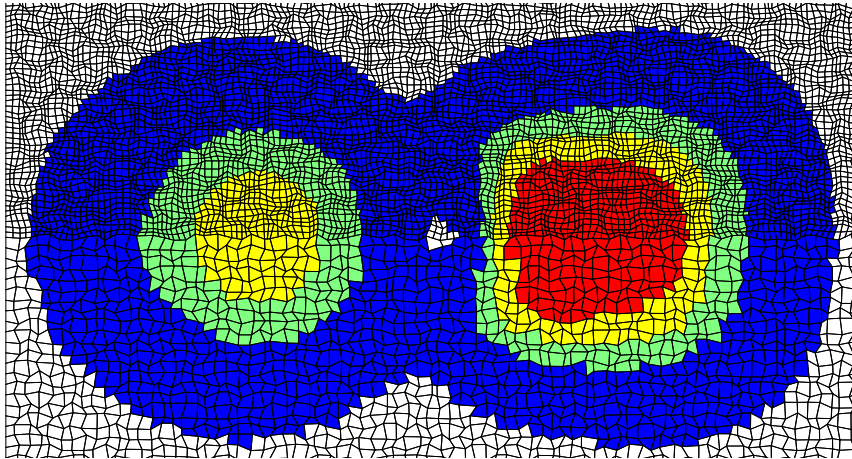


Figure 12. Transport of irregular functions - Solution at $t = \pi$ obtained with a locally refined mesh (part of the computational domain only). If $u \leq 0.01$, meshes are coloured in white - If $0.01 < u \leq 0.25$, in blue - If $0.25 < u \leq 0.5$, in green - If $0.5 < u \leq 0.75$, in yellow - If $0.75 < u$, in red.

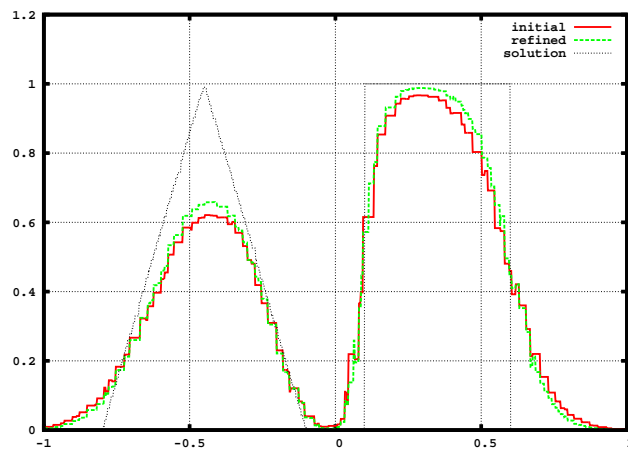


Figure 13. Transport of irregular functions - Value of the unknown along the x -axis, obtained with a locally refined mesh and with the quadrangular initial (*i.e.* before refinement) mesh.

The L^2 -norm of the difference between the numerical and continuous solution at $t = 1.2$ is given for several meshes (with a time step adjusted accordingly to have $\text{cfl} \approx 0.5$) in the following table.

initial mesh	40×40	80×80	160×160	320×320
time step	0.005	0.0025	0.001	0.0005
error (L^2 -norm)	0.0095	0.0028	0.00095	0.00042

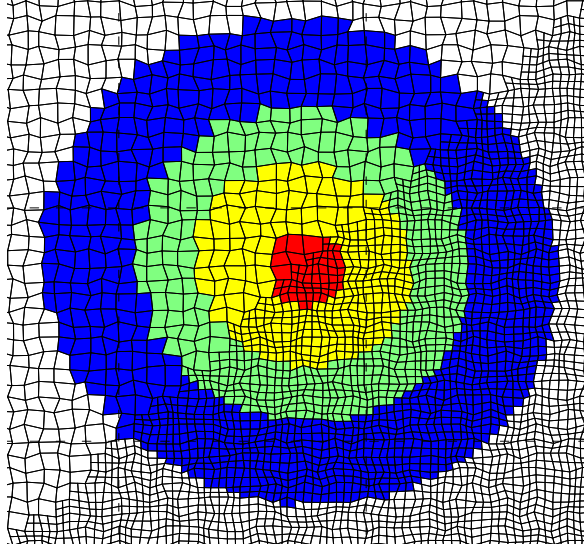


Figure 14. Convection-diffusion case - Solution obtained at $t = 1.2$ with a locally refined mesh (zoom on a part of the computational domain). If $u \leq 0.01$, meshes are coloured in white – If $0.01 < u \leq 0.05$, in blue – If $0.05 < u \leq 0.1$, in green – If $0.1 < u \leq 0.15$, in yellow – If $0.15 < u$, in red.

The convergence seems to be rather fast for coarse meshes, then slows down, the convergence rate however remaining greater than 1.

We now assess the capability of the scheme to work on a locally refined mesh. We start from the mesh of quadrangles obtained from the 80×80 mesh and cut in four sub-quadrangles the meshes located under the line $\mathbf{x}_2 = \mathbf{x}_1$. The result obtained at $t = 1.2$ in the upper left part of the computational domain (the part where the solution varies at that time) is plotted on Figure 14. We observe the absence of numerical perturbations at the edges where the mesh is non-conforming. In the upper part of the domain (*i.e.* $\mathbf{x}_2 > \mathbf{x}_1$), the numerical diffusion appears slightly larger, which is consistent with the fact that the mesh is coarser.

5. Conclusion

In this paper, we described a finite volume scheme for the solution of the advection-diffusion equation, which copes with almost arbitrary meshes. This scheme combines two ingredients:

- a discrete diffusion operator, which is both consistent and stable,
- a non-linear discrete transport operator using a prediction/limitation procedure, with a limitation step which ensures the satisfaction of a local maximum principle without invoking any geometrical argument.

The material presented here may be developed in several directions:

- first, the proposed limitation procedure may be used to complement any other existing algorithm, as a final step to ensure the local maximum principle without any restriction

on the mesh; doing so, the parameters should probably be tuned to limit as less as possible (*i.e.* to enlarge as much as possible the admissible interval for the value at the face),

- second, we payed no particular attention here to the reconstruction of the value at the face, and, especially for the transport of smooth functions, it is probably possible to design a more accurate evaluation, for instance using a least squares technique,
- last but not least, still for the transport of smooth functions, it is certainly preferable to switch to a second-order in time scheme.

In addition, the convection scheme presented here extends to variable density flows [2], *i.e.* to a balance equation for \bar{u} of the form $\partial_t(\rho\bar{u}) + \text{div}(\rho\bar{u}\mathbf{v}) - \text{div}(\kappa\nabla\bar{u}) = f$, where the density ρ and the velocity field \mathbf{v} are linked by the usual mass balance equation $\partial_t\rho + \text{div}(\rho\mathbf{v}) = 0$.

REFERENCES

1. L. Agelas and D. A. Di Pietro. Benchmark on Anisotropic Problems – a symmetric finite volume scheme for anisotropic heterogeneous second-order elliptic problems. In *FVCA5 – Finite Volumes for Complex Applications V*, pages 705–716. Wiley, 2008.
2. F. Babik, C. Lapuerta, J.-C. Latché, B. Piar, and S. Suard. ISIS: a computer code for fire simulation – Numerical schemes. *in preparation*, 2011.
3. T. Barth and M. Ohlberger. Finite volume methods: foundation and analysis. In *Encyclopedia of Computational Mechanics, Volume 1, Chapter 15*. John Wiley & Sons, 2004.
4. T. Buffard and S. Clain. Monoslope and multislope MUSCL methods for unstructured meshes. *Journal of Computational Physics*, 229:3745–3776, 2010.
5. C. Calgaro, E. Chane-Kane, E. Creusé, and T. Goudon. L^∞ -stability of vertex-based MUSCL finite volume schemes on unstructured grids: Simulation of incompressible flows with high density ratios. *Journal of Computational Physics*, 229:6027–6046, 2010.
6. E. Chénier, R. Eymard, and Herbin R. A collocated finite volume scheme to solve free convection for general non-conforming grids. *Journal of Computational Physics*, to appear, see also <http://hal.archives-ouvertes.fr>.
7. S. Clain. Finite volume L^∞ -stability for hyperbolic scalar problems. *submitted*, 2010.
8. S. Clain and V. Clauzon. L^∞ stability of the MUSCL methods. *Numerische Mathematik*, 116:31–64, 2010.
9. R. Eymard, T Gallouët, and R. Herbin. Discretisation of heterogeneous and anisotropic diffusion problems on general nonconforming meshes – SUSHI: a scheme using stabization and hybrid interfaces. *IMA Journal of Numerical Analysis*, 30:1009–1043, 2010.
10. R. Eymard and R. Herbin. A new collocated finite volume scheme for the incompressible Navier-Stokes equations on general non matching grids. *Comptes Rendus Mathématique. Académie des Sciences. Paris*, 344:659–662, 2007.
11. E. Godlewski and P.-A. Raviart. Numerical approximation of hyperbolic systems of conservation laws. Number 118 in Applied Mathematical Sciences. Springer, New York, 1996.
12. A. Harten. High resolution schemes for hyperbolic conservation laws. *Journal of Computational Physics*, 49:357–393, 1983.
13. ISIS. A CFD computer code for the simulation of reactive turbulent flows. <https://gforge.irsnn.fr/gf/project/isis>.
14. G. Manzini and A. Russo. A finite volume method for advection-diffusion problems in convection-dominated regimes. *Computer Methods in Applied Mechanics and Engineering*, 197:1242–1261, 2008.
15. PELICANS. Collaborative development environment. <https://gforge.irsnn.fr/gf/project/pelicans>.
16. PK. Sweby. High resolution schemes using flux limiters for hyperbolic conservation laws. *SIAM Journal on Numerical Analysis*, 21:995–1011, 1984.
17. Q.H. Tran. A scheme for multi-dimensional linear advection with accuracy enhancement based on a genuinely one-dimensional min-max principle. *In preparation*, 2010.
18. B. Van Leer. Towards the ultimate conservative difference scheme. ii. monotonicity and conservation combined in a second order scheme. *Journal of Computational Physics*, 14:361–370, 1974.